EVS27
Barcelona, Spain, November 17 - 20, 2013

Indirect Drive In-Wheel System for HEV/EV Traction

Y. Tang[1], J. J. H. Paulides, I. J. M. Besselink[2], F. Gardner[3], E. A. Lomonova
[1]*Electromechanics and Power Electronics Group, Department of Electrical Engineering, Eindhoven University of Technology, Den Dolech 2, 5612 AZ Eindhoven, the Netherlands, y.tang1@tue.nl*
[2]*Dynamics and Control Group, Department of Mechanical Engineering, Eindhoven University of Technology*
[3]*Teamwork Technology B.V., the Netherlands*

Abstract

In-wheel traction allows simplicity and freedom for the design of hybrid-electric/electric vehicle (HEV/EV). However, the in-wheel motor increases the unsprung mass and hence deteriorates ride comfort and reduces the road holding capability of the car. To solve these problems, this paper proposes an indirect drive in-wheel traction system including a light-weight in-wheel drive and a specially designed rear suspension. A prototype of the in-wheel drive is designed based on the vehicle model of Volkswagen (VW) Lupo 3L. The prototype analysis shows that the proposed in-wheel system gives a balanced distribution of the vehicle weight and thus improves ride comfort. Design principles of the electrical motor used for this in-wheel system is further investigated. By reducing the permanent magnet height, the field weakening capability of a 24-slot 8-pole surface permanent magnet synchronous motor is visibly improved.

Keywords: in-wheel traction, rear suspension, unsprung mass, motor design, field weakening

1 Introduction

With the rising concern on environmental issues, hybrid/electric vehicles (HEV/EV) have attracted an increasing interest from public and industry since the end of 20_{th} century. The fast developing technology of HEV/EV has also introduced a revolutionary traction concept to vehicles designers, namely in-wheel traction. By putting electrical motors in the wheels, the drivetrain is greatly simplified. Mechanical axes can thus be removed, which creates extra space for the cargo and reduces the total weight of the vehicle [1], [2] (Fig. 1a). These advantages of simplicity and freedom make the in-wheel traction a preferable traction mode for vehicle designers.

Research and development of advanced in-wheel motors and in-wheel traction systems are thus intensively carried out [3], [4], [5], [6]. The company E-Traction designed a direct drive outer-rotor motor, namely $TheWheel^{\text{TM}}$ (Fig. 1b) [7]. Protean Electric developed an in-wheel electric drive system, namely $ProteanDrive^{\text{tm}}$ (Fig. 1c) [8]. Ford and Schaeffler demonstrated a Fiesta-based $eWheelDrive^{\text{TM}}$ car powered by independent electric motors in each of the rear wheels (Fig. 1d), together delivering 40kW, peak and 33kW, continuous power [9].

However, in most existing in-wheel traction systems, the electrical motor is directly driving the wheel, as shown in Fig. 1b. This direct drive concept of the in-wheel traction greatly raises the torque requirement for the electrical motor design. At certain operation points, such as curb climbing, the torque requirement becomes uneconomical or even impractical and thus limits the vehicle performance. In addition, high torque requirement leads to the requirement of large volume for the in-wheel motor, resulting in

(a) (b)

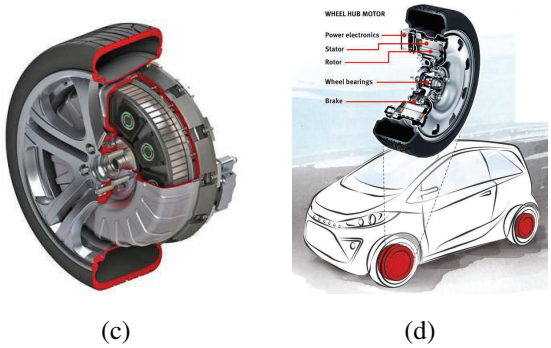

(c) (d)

Figure 1: In-wheel traction - a) An electric truck with large cargo; b) $TheWheel^{TM}$, ETraction; c) $ProteanDrive^{TM}$, Protean Electric; d) $eWheelDrive^{TM}$, Ford and Schaeffler

large additional unsprung mass. The increased unsprung mass can be problematic because it potentially deteriorates ride comfort and reduce road holding capability of the car [10].

Problems caused by large unsprung mass are further explained in Section 2. To improve the vehicle performance of HEV/EV with in-wheel traction, this paper proposes an indirect drive in-wheel traction system including a light-weight in-wheel drive and a specially designed rear suspension system, based on the vehicle model of VW Lupo 3L. The structure of this light-weight in-wheel drive is described in Section 3, in which the electrical motor is indirectly driving the wheel through a gearbox. By this means the required torque for the motor is reduced and the mass of the in-wheel drive is minimized. Principles of selection and design of the electrical motor for the proposed in-wheel drive is discussed in Section 4. A special design of the rear suspension system is further introduced in Section 5.

2 Problems of in-wheel traction

Problems of in-wheel traction due to the increased unsprung mass is revealed by the oscillation model of an electrical vehicle, as shown in Fig. 2. In this model, the vehicle mass above the suspension system is represented as sprung mass, while the mass below the suspension system is represented as unsprung mass. When the unsprung mass increases, the unsprung-to-sprung mass ratio increases. Variation of this ratio leads to changes in three criteria used for assessing the vehicle performance, which are:

- The transmissibility ratio
  - the response of the sprung mass to the excitation from the road
  - used for assessing the ride comfort of a vehicle
- The suspension travel ratio
  - the ratio of the maximum relative displacement between the sprung and unsprung mass to the amplitude of the road input
  - used for assessing the space required to accommodate the suspension spring.
- The dynamic tyre deflection ratio
  - the ratio of the maximum relative displacement between the unsprung mass and the road surface to the amplitude of the road input
  - used for assessing the handling and safety of the vehicle.

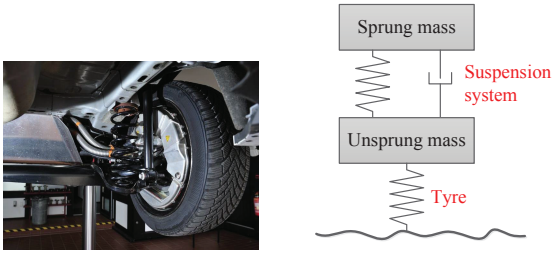

(a) (b)

Figure 2: Oscillation model of quarter car - a)$eWheelDrive^{TM}$ with wheel suspension; b) oscillation model

The general effect of an increased unsprung-to-sprung mass ratio on the three criteria are shown in Fig. 3. In the frequency range between the natural frequency of the sprung mass and that of the unsprung mass, all three criteria increases with the unsprung-to-sprung mass ratio increases. This suggests a reduced ride comfort, an increased accommodation space for the suspension spring, and an increased difficulty in handling the vehicle [11].

To solve the problems caused by increased unsprung mass, several companies proposed and developed various in-wheel drives that contain active suspension systems, such as the active wheel drive in-wheel motor of Michelin (Fig. 4a) [12] and the eCorner of Siemens (Fig. 4b) [13]. Moreover, Bridgestone invented a dynamic damping in-wheel drive, in which the shaftless motor is suspended using flexible coupling. It is claimed that by this means the vibration input from the road irregularities is cancelled by

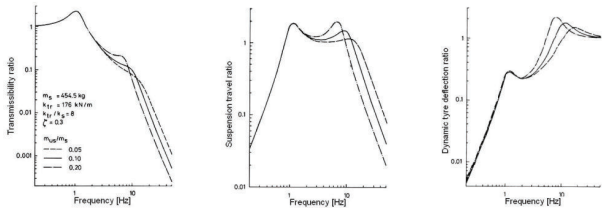

(a) (b) (c)

Figure 3: Effect of unsprung-to-sprung mass ratio on: a) the transmissibility ratio; b) the suspension travel ratio; c) the dynamic tyre deflection ratio. [11]

the vibration of the motor, resulting in an improved road-holding performance and ride comfort (Fig. 4c) [14]. However, active suspension consumes energy, which is scarce in a battery electric vehicles (BEV). Besides, full electric active suspensions are not yet well developed and usually heavy, while hydraulic active suspensions are less compatible with EVs.

(a) Michelin active wheel

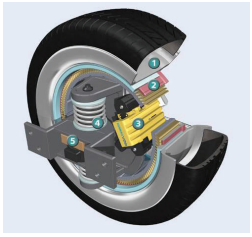

(b) Siemens eCorner

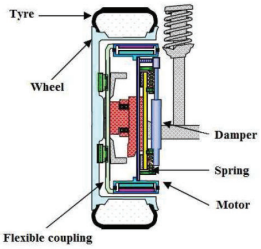

(c) Bridgstone's dynamic-damping in-wheel drive

Figure 4: Advanced in-wheel drives dealing with the problem of increased unsprung mass

3 Light-weight in-wheel drive

A light-weight in-wheel drive is proposed to minimize the unsprung mass of HEV/EV with in-wheel traction, shown in Fig 5a. In this drive, the electrical motor is indirectly driving the wheel through a gearbox, thus the required torque for the electrical motor is reduced, shown in Fig 5b, leading to reduction on the motor volume and mass.

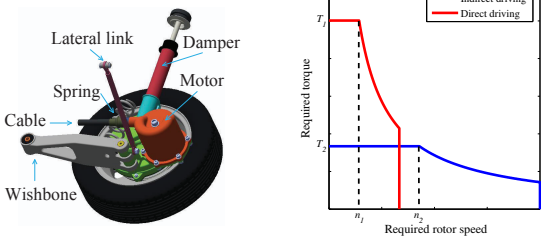

(a) (b)

Figure 5: Light-weight in-wheel drive a) the structure and b) torque-speed requirements for electrical motors in direct drive and indirect drive in-wheel traction systems.

A prototype (Fig. 6a) is designed and manufactured based on the specification of VW Lupo 3L (Fig. 6b), in which the gear ratio is 14.76. Parameters of this car are summarized in Table. 1. The car is driven by two in-wheel drives in the rear wheels. Based on this design, the torque and speed requirements for the electrical motor of this indirect drive in-wheel system are compared to that in a direct drive in-wheel system, shown in Table 2. It can be seen that by implementing the gearbox, the required torque of the electrical motor is significantly reduced. It is also shown that the maximum power of this VW Lupo 3L is comparable to the Fiesta-based eWheelDrive car developed by Ford and Schaeffler. Therefore, it is reasonable to compare the masses of the two different drives.

Table 1: Vehicle parameters of VW Lupo 3L

Description	Symbol	Value
Total mass (including driver)	m	1100kg
Wheel diameter	D_{w}	0.556m
Frontal vehicle area	S_{F}	1.97m^2
Kinetic friction coefficient	μ	0.0085
Drag coefficient	C_{D}	0.29
Maximum mechanical power	P_{max}	40kW

In the demonstrated Fiesta-based eWheelDrive car, the total mass of the wheel hub drive is 53kg. While the total mass of the prototype of this light-weight in-wheel drive is 31.5kg, in which the mass of the motor is 13.8kg. Therefore, the proposed drive is 40.6% lighter than the eWheelDrive.

4 Electrical motor design

4.1 Electrical motor type selection

The electrical motor designed for this light-weight in-wheel drive needs to have a high torque

Table 2: Torque-speed requirements for the in-wheel motor in different drive modules

Corner cases	Direct driving		Indirect driving		Power P (kW)
	Torque T (Nm)	Speed n (rpm)	Torque T (Nm)	Speed n (rpm)	
140km/h @ 0%	85.0	1336	5.8	19717	11.9
130km/h @ 0%	75.0	1240	5.1	18309	9.7
80km/h @ 10%	187.0	763	12.7	11267	14.9
50km/h @ 15%	246.5	477	16.7	7042	12.3
15km/h @ 30%	448.0	143	30.4	2113	6.7
0 - 100 km/h (14s)	494.5	0 - 954	33.5	0 - 14084	0 - 20

(a) Prototype

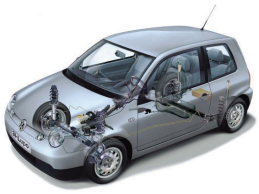

(b) VW Lupo 3L

Figure 6: Prototype of the light-weight in-wheel drive for Volkswagen Lupo 3L.

density with a wide constant power speed range (CPSR). Table 3 shows the torque density and speed ratio of different types of electrical motors [15]. It can be seen that permanent magnet synchronous motor (PMSM) has the highest torque density and thus is a strong candidate for this application.

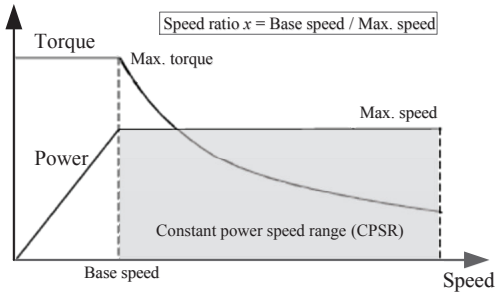

Figure 7: Constant power speed region of an electrical motor.

Table 3: Torque densities for different motor types

Machine type	Torque density (Nm/m^3)
Permanent magnet synchronous motor	28860
Induction motor	4170
Switched reluctance motor	6780

4.2 PMSM design for wide CPSR

However, CPSR of PMSM is highly depending on the field weakening capability, which is inherently decided by the motor design. In the PMSM design, two parameters are related to the fielding weakening capability, which are the normalised PM flux linkage Ψ_{mn} and the saliency ratio ξ [17].

One the one hand, the normalised PM flux linkage Ψ_{mn} is calculated as:

$$\Psi_{\mathrm{mn}} = \frac{\Psi_{\mathrm{m}}}{\Psi_{\mathrm{b}}}, \tag{1}$$

in which Ψ_{m} is the flux linkage produced by permanent magnet and Ψ_{b} is the total flux linkage at the base speed, as indicated in Fig. 8. A high saliency ratio

Figure 9 shows the relation between the nominal rotor speed ω_{n} and the nominal output power P_{n} with different values of the permanent magnet flux linkage Ψ_{mn}. It can be seen that the maximum CPSR is achieved when Ψ_{mn} is smaller than 0.71.

On the other hand, the saliency ratio ξ is defined as:

$$\xi = \frac{L_{\mathrm{d}}}{L_{\mathrm{q}}}, \tag{2}$$

in which L_{d} and L_{q} are inductances in the direct- and quadrature-axis.

In PMSM, the electromagnetic torque can be calculated as:

$$T_{\mathrm{em}} = \frac{3p}{2}[\Psi_{\mathrm{m}} i_{\mathrm{q}} - (L_{\mathrm{d}} - L_{\mathrm{q}}) i_{\mathrm{d}} i_{\mathrm{q}}] \tag{3}$$

$$= \frac{3p}{2}[\Psi_{\mathrm{m}} i_{\mathrm{q}} - (\xi - 1) L_{\mathrm{d}} i_{\mathrm{d}} i_{\mathrm{q}}], \tag{4}$$

in which the first term in the square bracket represents the Lorentz torque component and the second term is the reluctance torque component.

During the field weakening, the Lorentz torque reduces due to reduction on i_{q}. However, due

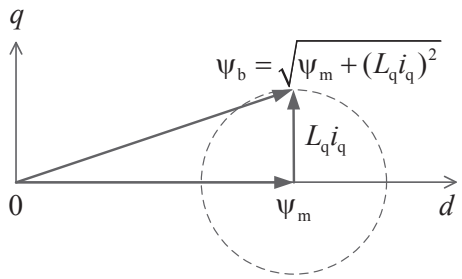

(a) Non-salient PMSM

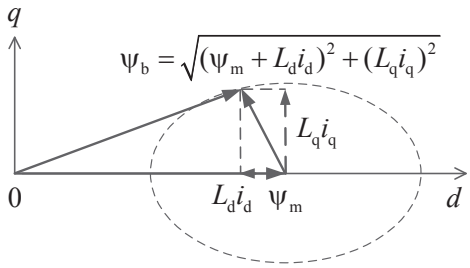

(b) Salient PMSM

Figure 8: Phasor diagram of flux linkages in permanent magnet synchronous motors.

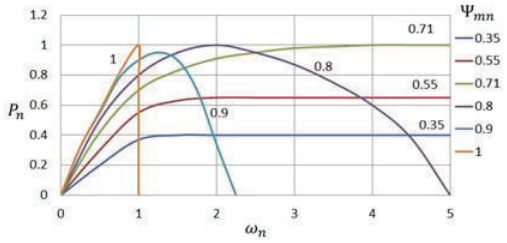

Figure 9: Impact of the nominal PM flux linkage Ψ_{mn} on the constant power speed range of permanent magnet synchronous motors.

to the appearance of a negative d-axis current, i.e. $i_d < 0$, the reluctance torque increases when $\xi < 1$, i.e. $L_q < L_d$ and thus compensates the reduced Lorentz torque. This compensation effect can be enhanced with increasing the saliency ratio ξ, hence the CPSR is extended.

Therefore, from the design point of view, the field weakening capability of PMSM can be improved in following aspects:

- Saliency Salient machines usually give a high saliency ratio. This ratio can be further increased using specific design for the rotor structure.
- Magnet height By reducing the height of magnet poles, the PM flux linkage can be reduced, hence the nominal PM flux linkage is also reduced, leading to a wider CPSR.
- Winding topology Compared to distributed windings, machines with concentrated windings have considerably higher inductance, mainly due to higher slot leakage, hence a higher rated flux linkage and a lower nominal PM flux linkage. Therefore, they have a wider CPSR.

4.3 Design optimization

In this paper, the design methods in extending the CPSR of PMSM are used to optimize the design of a 24-slot 8-pole surface PMSM, shown in Fig. 10 for the proposed light-weight in-wheel drive. The original design of this PMSM, denoted as M_I, is summarized in Table 4.

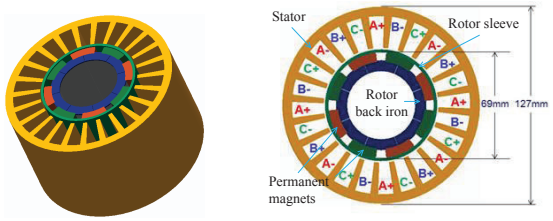

(a) (b)

Figure 10: Design layout of the 24-slot 8-pole permanent magnet synchronous motor: a) 3D structure; b) Cross-section.

Table 4: Motor parameters

Description	Symbol	Value	Unit
Stator slot number	N_s	24	-
Rotor pole number	p	8	-
Coil turn number (per slot)	N_t	12	-
Stack length	L	76.4	mm
Stator outer diameter	D_{so}	127.3	mm
Rotor outer diameter	D_{ro}	69.1	mm
Airgap length	δ	3.0	mm
Magnet height	h_m	6.0	mm

The torque-speed characteristic of this design at 150V supply voltage is shown in Fig. 11. To generate the maximum required torque, 88A current is needed. This current requirement can be reduced by increasing the number of coil turns in a stator slot N_t. When N_t is doubled to 12 turns, the required current for the maximum torque is reduced to 44A, which is half of that in M_I. However, in this case the base speed is also reduced to half of the original value as the

induced back-EMF is doubled.

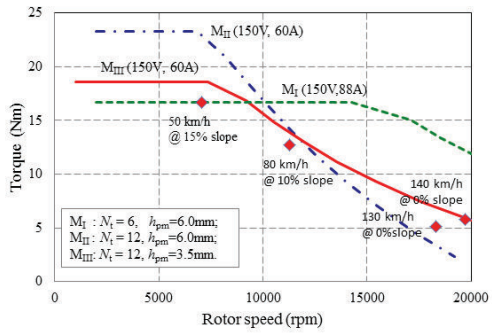

Figure 11: Torque-speed characteristics of the permanent magnet synchronous motor in different design versions M_I, M_{II}, and M_{III}.

The advantage of this adapted version of design, denoted as M_{II}, is that the sizes of the battery and power electronics modules are reduced. However, the problem is that with 150V supply voltage and 44A phase current, this design cannot meet the torque-speed requirements for the operation points above the base speed. Even when the phase current is increased to 60A, the torque-speed profile of M_{II} still cannot cover the two operation points at maximum vehicle speeds, as the blue dot-dashed curve shows in Fig 11. This implies room to improve the field weakening capability of this design.

A simple method without changing the winding topology and rotor structure is adjusting the magnet height hpm. By reducing hpm from 6mm to 3.5mm, the new version of design, denoted as M_{III}, provides a torque-speed profile that is able to cover all required operation points with 150V supply voltage and 60A phase current, as the red solid curve shows in Fig. 11.

5 Rear suspension design

The rear suspension of VW Lupo 3L is shown in Fig. 12, in which the two trailing arms are welded to a twistable cross-member and the forward mounting of the arms are pivoted on the vehicle body [16]. For a HEV/EV, this rear suspension interferes the battery box, as shown in Fig. 13a. It splits the battery pack into two parts and hence complicates the access to the battery pack. For example, during servicing of the battery pack, suspension components need to be first removed.

A rear suspension that does not interfere with the battery box is thus preferred, as shown in Fig 13c. An additional advantage of this design is that more weight is shifted to the rear due to the new design and placement of the battery box, shown in Fig 14. The weight distributions in

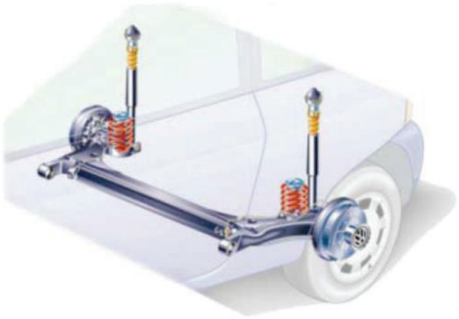

Figure 12: Rear suspension of VW Lupo 3L.

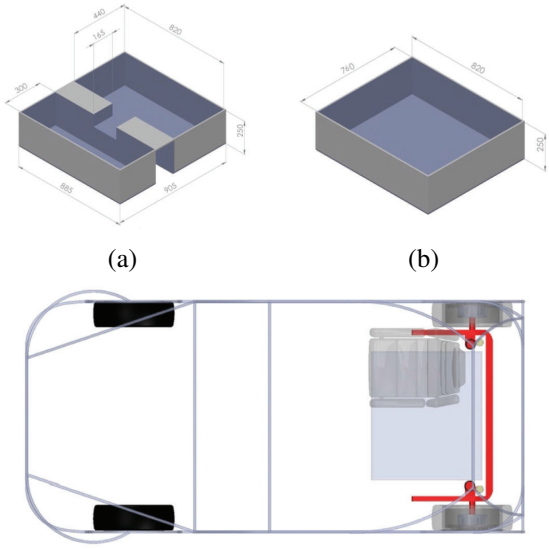

(a) (b)

(c)

Figure 13: Illustration of the new rear suspension design: a)The battery box with the original rear suspension in VW Lupo 3L; b) The battery box with the new rear suspension; c)Placement of the battery box with the new rear suspension.

the original Lupo 3L, the Lupo-based electrical car using conventional rear suspension, denoted as Lupo EL, and the Lupo-based electrical car using the new rear suspension, denoted as Lupo EL2, are compared in Table 5 [18]. It can be seen that Lupo 3L and Lupo EL are front heavy cars, while in Lupo EL2 the weight is more evenly distributed and slightly shifted to the rear. This weight shift increases the sprung mass above the rear suspension, which compensates the ride comfort influenced by the increased unsprung mass. It is worth mentioning that the suspension mass is a part of the unsprung mass. Therefore, light materials, such as carbon fibre, are recommended for the manufacture of the suspension components.

Table 5: Mass distribution of the three cars

	Lupo 3L	Lupo EL	Lupo EL2
Mass on the front axle	615.5kg	675kg	526.2kg
Mass on the rear axle	385.5kg	545kg	625.8kg
Total mass	1001kg	1220kg	1152kg
Weight distribution ($m_{\text{front}}/m_{\text{rear}}$)	64:36	58:42	46.5:53.5

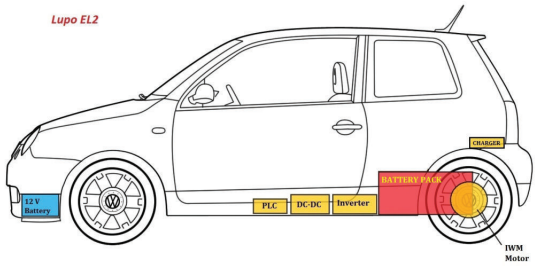

Figure 14: Configuration of Lupo EL2.

6 Conclusions

In-wheel traction is a preferable traction mode for the design of hybrid-electric/electric vehicles (HEV/EV) because it simplifies the drivetrain structure and enlarges the cargo space. However, it also increases the unsprung mass, leading to a reduced ride comfort, an increased accommodation space required for the suspension spring, and an increased difficulty in handling the vehicle.

To solve these problems, this paper proposes a light-weight in-wheel drive in which the electrical motor is indirectly driving the wheel through a gearbox. By this means the torque requirement of the electrical motor is significantly reduced, resulting in a reduced total mass of the in-wheel drive. Permanent magnet synchronous motor (PMSM) is selected as a suitable type of motors for this in-wheel drive due to its high torque density. However, a wide constant power speed range (CPSR) is also required for the traction of HEV/EV. Hence, design methods in extending the speed range of PMSM are studied and implemented into the optimization of a motor design for the proposed in-wheel drive. By reducing the magnet height, the fielding weakening capability of the 24-slot 8-pole surface PMSM is visibly improved, resulting in reduction on the size of battery and power electronics modules.

Furthermore, a special design of the rear suspension that allows easy access to the battery pack is analysed. This design also shifts more weight of the vehicle to the rear, which increases the rear sprung mass and thus balances the increased unsprung mass of the rear wheels.

7 Acknowledgments

The authors acknowledge the supports from Teamwork Technology, Lightweight Structures, Molenaar Strategie, Wolters Engineering, and Vredestein.

References

[1] E. Lomonova, E. V. Kazmin, Y. Tang, J. J. H. Paulides, *In-wheel PM motor: compromise between high power density and extended speed capability*, COMPEL: The International Journal for Computation and Mathematics in Electrical and Electronic Engineering, 30(1), 98-116, 2011.

[2] Z. Q. Zhu, D. Howe, *Electrical Machines and Drives for Electric, Hybrid, and Fuel Cell Vehicles*, Proceedings of the IEEE, 95(4), 746 - 765, April 2007.

[3] K. M. Rahman, N. R. Patel, T. G. Ward, J. M. Nagashima, F. Carcchi, F. Crescimbini, *Application of direct drive wheel motor for fuel cell electric and hybrid electric vehicle propulsion system*, IEEE Transaction on Industry Application, 42(5), 1185 - 1192, 2004.

[4] W. Fei, P. C. K. Luk, K. Junipun, *A new axial flux permanent magnet segmented-armature-torus machine for in-wheel direct drive applications*, Power electronics specialists conference (PESC), Cranfield University, 2008.

[5] O. Mokhiamar, M. Abe, *Simulataneous optimal distribution of lateral and longitudinal tire forces for the model following control*, ASME Journal of Dynanic Systems, Measurement, and Control, Vol. 126, 753 - 763, 2004.

[6] Y. Hori, *Future vehicle driven by electricity and control - research on four-wheel-motored "UOT Electrica March II"*, IEEE Transaction on Industrial Electronics, 51(5), 954 - 962, 2004.

[7] *TheWheel - Product introduction*, http://www.e-traction.eu/the-wheel/product-introduction, accessed in 2011.

[8] *Protean drive*, http://www.proteanelectric.com, accessed in 2011.

[9] *Ford and Schaeffler demonstrate Fiesta-based e-WheelDrive car; follow-up research project in the works*, http://www.greencarcongress.com/2013/04/ewheel-20130426.html, accessed in 2011.

[10] R. Vos, I. J. M. Besselink, H. Nijmeijer, *Influence of in-wheel motors on the ride comfort of electric vehicles*, Proceeding of the Proceedings of the 10_{th} International Symposium on Advanced Vehicle Control (AVEC10), pp. 835-840, Loughborough, United Kingdom, 22-26 August 2010.

[11] R. Vos. *Influence of in-wheel motors on the ride comfort of electric vehicle*, master's thesis, Eindhoven University of Technology, the Netherlands, 2010.

[12] *Michelin reinvents the wheel*, http://www.michelin.co.uk, accessed in 2011.

[13] *eCorner*, http://www.siemens.com, accessed in 2011.

[14] *Bridgestone Dynamic-Damping In-wheel Motor Drive System*, http://www.bridgestone.eu, accessed in 2011.

[15] M. Ehsani, Y. Gao, J. M. Miller, *Hybrid Electric Vehicles: Architecture and Motor Drives* , Proceedings of the IEEE, 95(4), 719 - 728, April 2007.

[16] J. Reimpell, H. Stoll, J. W. Belzler, *The Automotive Chassis: Engineering Principles.*, No. ISBN: 0-7506-5054-0, Butterworth-Heinemann, 2001.

[17] W. L. Soong, T. J. E. Miller, *Field weakening performance of brushless synchronous AC motor drives*, IEE Proceedings-Electrical Power Application, 141(6), November 1994.

[18] A. D. George. *Suspension design and analysis for a VW Lup*, master's Thesis, Eindhoven University of Technology, the Netherlands, 2011.

Authors

Yang Tang received the B.Sc. and M.Sc. degrees in Electrical Engineering from Zhejiang University, China in 2003 and 2006, respectively. Since 2007, he has been working as a researcher at Eindhoven University of Technology (TU/e), the Netherlands. He currently works towards the PhD degree at the Electromechanics and Power Electronics (EPE) Group of TU/e. His research activities are focused on pre-biased variable field electrical machines.

Johannes J. H. Paulides received the B.Eng. degree from the Technische Hogeschools-Hertogenbosch in 1998 and the M.Phil. and Ph.D. degrees in Electrical and Electronical Engineering from the University of Sheffield in 2000 and 2005, respectively. Since 2005, he has been working at Eindhoven University of Technology, the Netherlands. He currently holds a part-time Assistant Professor position within the Electromechanics and Power Electronics Group. Simultaneously, he is a director of various SMEs related to his field of interest. His research activities span all facets of electrical machines, however, in particular permanent magnet excited machines for more electric applications.

Igo Besselink is an assistant professor at the Eindhoven University of Technology, department of Mechanical Engineering, Dynamics and Control. Research activities include tyre modelling, vehicle dynamics and electric vehicles

Fred Gardner started his career as an electronic engineer but broadened his skills into mechanical engineering and management of the innovation process. Since 1993 he has become the director/owner of Teamwork Technology B. V. in the Netherlands. His activity includes innovation and development of new business with a focus on sustainable energy.

Elena A. Lomonova (M'04-SM'07-F'10) was born in Moscow, Russia. She received the M.Sc. (cum laude) and Ph.D. (cum laude) degrees in electromechanical engineering from the Moscow State Aviation Institute, in 1982 and 1993, respectively. She currently holds a Professor position with the Department of Electrical Engineering, Eindhoven University of Technology, Eindhoven, the Netherlands. She has worked on electromechanical actuator design, optimization, and the development of advanced mechatronics systems.